

CO₂-induced seawater acidification affects physiological performance of the marine diatom *Phaeodactylum tricornerutum*

Y. Wu¹, K. Gao¹, and U. Riebesell²

¹State Key Laboratory of Marine Environmental Science, Xiamen University, Xiamen, China

²Leibniz Institute of Marine Sciences (IFM-GEOMAR), Kiel, Germany

Received: 25 April 2010 – Published in Biogeosciences Discuss.: 25 May 2010

Revised: 8 August 2010 – Accepted: 25 August 2010 – Published: 24 September 2010

Abstract. CO₂/pH perturbation experiments were carried out under two different *p*CO₂ levels (39.3 and 101.3 Pa) to evaluate effects of CO₂-induced ocean acidification on the marine diatom *Phaeodactylum tricornerutum*. After acclimation (>20 generations) to ambient and elevated CO₂ conditions (with corresponding pH values of 8.15 and 7.80, respectively), growth and photosynthetic carbon fixation rates of high CO₂ grown cells were enhanced by 5% and 12%, respectively, and dark respiration stimulated by 34% compared to cells grown at ambient CO₂. The half saturation constant (*K_m*) for carbon fixation (dissolved inorganic carbon, DIC) increased by 20% under the low pH and high CO₂ condition, reflecting a decreased affinity for HCO₃⁻ or/and CO₂ and down-regulated carbon concentrating mechanism (CCM). In the high CO₂ grown cells, the electron transport rate from photosystem II (PSII) was photoinhibited to a greater extent at high levels of photosynthetically active radiation, while non-photochemical quenching was reduced compared to low CO₂ grown cells. This was probably due to the down-regulation of CCM, which serves as a sink for excessive energy. The balance between these positive and negative effects on diatom productivity will be a key factor in determining the net effect of rising atmospheric CO₂ on ocean primary production.

1 Introduction

The ongoing increase of atmospheric CO₂ concentration has aroused great attention, regarding its biological, environmental and climatological effects (Doney et al., 2009). In the ocean, CO₂ absorption by seawater leads to increased *p*CO₂ and bicarbonate concentration and decreased pH and carbonate ion concentration. For the past century, more than one third of the anthropogenic CO₂ released to the atmosphere has been absorbed by the ocean (Sabine et al., 2004), leading to a global scale drop of pH by 0.1 (30% increase in [H⁺]). In a business as usual CO₂ emission scenario, oceanic uptake of CO₂ will acidify the surface ocean by 0.3–0.4 pH units ([H⁺] increase by 100–150%) by the end of this century (Caldeira and Wickett, 2003). Calcifying organisms, such as coccolithophorids (Riebesell et al., 2000), corals (Hoegh-Guldberg et al., 2007), coralline algae (Gao et al., 1993), and mollusks (Orr et al., 2005) have been shown to be most sensitive to seawater acidification because of its adverse effects on the formation of the aragonite or calcite armors protecting their bodies. Respiration of marine organisms (Crawley et al., 2010), as well as sound absorption in the ocean (Hester et al., 2008), can also be affected by seawater acidification. However, increased CO₂ availability may be beneficial for marine phytoplankton. Due to the low affinity of their carboxylating enzyme (Rubisco) for CO₂ (Badger et al., 1998), rising CO₂ could lead to enhanced phytoplankton growth and photosynthetic carbon fixation (Riebesell et al., 1993; Hein and Sand-Jensen, 1997).



Correspondence to: K. Gao
(ksgao@xmu.edu.cn)

Diatoms, contributing about half of the marine primary production, are known to actively take up both CO₂ and bicarbonate for photosynthesis to counteract the limited availability of CO₂ in seawater (Burkhardt et al., 2001; Rost et al., 2003). Such CO₂ concentrating mechanisms (CCMs) also exist widely in other algal species (Giordano et al., 2005). From this point of view, therefore, the atmospheric CO₂ rise and associated increase in seawater *p*CO₂ may not be critically important in affecting marine primary production (see review by Giordano et al. 2005). However, it is known that the operation of CCMs can be down-regulated under extremely high CO₂ conditions up to 5% (Xiang et al., 2001). Such enrichment of CO₂ to about hundred times of the present CO₂ level can hardly reflect future-projected chemical changes in the carbonate system of seawater. Therefore, ecological implications of the ongoing ocean acidification can not derived from these studies. Although recent studies (Burkhardt et al., 2001; Rost et al., 2003) have shown that diatoms' CCMs could be responsive to ocean acidification under projected CO₂ emission scenarios, little is known about their physiological responses to the change in the seawater carbonate system under elevated CO₂ concentration.

We hypothesize that under ocean acidification diatoms may increase their metabolic demand for energy to balance the external pH decrease. At the same time, adjusting their capability to actively take up inorganic carbon (Ci) may save some energy from down-regulating CCM operation. Together these responses may lead to different physiological sensitivities to changes in light and Ci concentrations. In this study, we used *Phaeodactylum tricornerutum*, a model diatom species that has been intensively studied in previous works, to understand the physiological mechanisms underlying observed CO₂/pH sensitivities, while the completely sequenced genome (<http://genome.jgi-psf.org/Phatr2/Phatr2.home.html>) permits follow-up studies relying on the genetic information.

2 Materials and methods

2.1 Cells and culture condition

Phaeodactylum tricornerutum (CCMA 106) was isolated from the South China Sea (SCS) in 2004 and obtained from the Center for Collections of Marine Bacteria and Phytoplankton (CCMBP) of the State Key Laboratory of Marine Environmental Science (Xiamen Univ.). The cells were inoculated in artificial seawater prepared according to Aquil medium (Morel et al., 1979) and cultured semi-continuously and axenically for at least 20 generations before use in experiments. The culture medium was renewed every 24 h to maintain the cell concentration within a range of 8×10^4 – 3×10^5 cells mL⁻¹. Aeration was provided at a flow rate of 350 mL min⁻¹ with ambient air of 39.3 Pa (388 ppmv) CO₂ (set as control) or with air enriched with CO₂ to 101.3 Pa (1000 ppmv)

(“business-as-usual” emission scenario in the early next century). The cultures were illuminated with cool white fluorescent tubes at photon flux densities of 120 μmol m⁻² s⁻¹ (14:10 light:dark) and 20°C.

2.2 CO₂ perturbation and seawater carbonate system

The artificial seawater was prepared to contain dissolved inorganic carbon, nitrate, phosphate and silicate concentrations of 2100, 100, 10, and 100 μmol kg⁻¹, respectively. Target pH (*p*CO₂) in the cultures and the fresh medium were achieved by bubbling pre-mixed air-CO₂ mixtures (39.3 ± 1.1 and 101.3 ± 3.0 Pa) (as recommended in Barry et al., 2010) within a plant growth CO₂ chamber (HP1000G-D, Ruihua), which controls the high CO₂ level with a variation of less than 3%. The concentration of DIC was measured before and after the renewal of the culture using a DIC analyzer (AS-C3, Apollo Scitech) that employs an infrared gas detector (Li-Cor 7000, Li-Cor). The pH changes were determined with a pH meter (Benchtop pH510, OAKTON) which was calibrated with standard National Bureau of Standards (NBS) buffer solution (Hanna). The nutrient drawdown was estimated from daily integrated carbon fixation based on the reported ratios of *N* or *P* to *C* (Burkhardt et al., 1999) and silica content (Conley et al., 1989). Subsequently, other parameters of the carbonate system were computed with CO2SYS software (Lewis and Wallace, 1998) based on the known values of DIC, pH, salinity, and nutrients, and cross-checked with DIC and *p*CO₂, the equilibrium constants *K*₁ and *K*₂ for carbonic acid dissociation after Roy et al. (1993), and *K*_B for boric acid after Dickson (1990).

2.3 Chlorophyll fluorescence measurements

To examine immediate photochemical responses of the cells grown at different levels of pH/CO₂ to changes in seawater carbonate system, the low-pH (high CO₂, H-C) grown cells were transferred to the high-pH (low CO₂, L-C) medium, and vice versa. The cells grown at the high pH and then transferred to the low pH medium for the measurements were expressed as L-C-H-C; contrarily, it was defined as H-C-L-C. In the middle of the light period, cells were harvested by centrifuge (Universal 320R, Hettich) at 4000 g and 20°C for 10 min, then re-suspended in 50 mmol L⁻¹ Tris buffered medium (pH 7.80 and pH 8.15) with a final cell density of 2 – 3×10^4 mL⁻¹. This cell suspension was transferred into transparent plastic syringes (20 mL) to avoid any leakage of CO₂ from the culture medium. Fluorescence induction curves were measured after 10 min dark adaptation with a xenon-pulse amplitude modulated fluorometer (XE-PAM, Walz). The actinic light levels were set at 120 or 840 μmol photons m⁻² s⁻¹ to examine non-photochemical quenching. The saturating pulse was applied at 5000 μmol photons m⁻² s⁻¹ for 0.8 s. Each measurement of the induction curve lasted for about 260 s. For the measurement of rapid light curve

(RLC), the re-suspended cells were incubated at $120 \mu\text{mol photons m}^{-2} \text{s}^{-1}$ and 20°C for 10 min to avoid induction effects on the photosystems caused by quasi-dark adaptation during manipulation. The RLCs were determined at 8 different PAR levels (84, 125, 185, 285, 410, 600, 840, and $1200 \mu\text{mol photons m}^{-2} \text{s}^{-1}$), each of which lasted for 10 s. Non-photochemical quenching (NPQ) was calculated as: $\text{NPQ} = (F_m - F_m') / F_m'$, where F_m represents the maximum fluorescence yield after dark adaptation, F_m' the maximum fluorescence yield determined at the actinic light levels. The relative electron transport rate (rETR, arbitrary unit) was assessed as: $\text{rETR} = \text{yield} \times 0.5 \times \text{photon flux density (PFD)}$, where the yield represents the effective quantum yield of PSII (F_v / F_m'); the coefficient 0.5 takes into account that roughly 50% of all absorbed quanta reach PSII; and PFD is the actinic light intensity ($\mu\text{mol m}^{-2} \text{s}^{-1}$).

2.4 Determination of Ci utilization and K_m

The cells harvested and re-suspended at a final density of $2\text{--}3 \times 10^4 \text{ mL}^{-1}$ were dispensed into 15 mL quartz tubes and inoculated with $50 \mu\text{L-}2.5 \mu\text{Ci}$ (92.5 kBq) of ^{14}C labeled sodium bicarbonate (Amersham). The samples were then placed in a water bath for temperature control at $20 \pm 0.1^\circ\text{C}$ using a recirculating cooler (CTP-3000, Eyela) under the same PAR level as in culture ($120 \mu\text{mol photons m}^{-2} \text{s}^{-1}$) for 2 h. After the incubations, cells were collected on Whatman GF/F glass fiber filters (25 mm), which were placed into 20 mL scintillation vials, exposed to HCl fumes overnight to expel non-incorporated ^{14}C and dried (45°C). Then 3 mL scintillating cocktail (Hisafe 3, Perkin-Elmer) was added into each vial and the assimilated ^{14}C was counted with a liquid scintillation counter (Tri-Carb 2800TR, Perkin-Elmer).

The relationship of photosynthesis vs. DIC concentrations was determined by re-suspending the cells at ca. 1.5×10^5 (for C-fixation) or $2\text{--}3 \times 10^4 \text{ mL}^{-1}$ (for RLC) in DIC free tris buffered medium (pH 8.15) and injecting sodium bicarbonate solution at final DIC concentrations between $50\text{--}4000 \mu\text{mol L}^{-1}$. Then RLC was measured as mentioned above, while the measurements of photosynthetic carbon fixation were initiated by inoculating $50 \mu\text{L-}2.5 \mu\text{Ci}$ (92.5 kBq) of ^{14}C , and immediately incubating (for 20 min) at $400 \mu\text{mol photons m}^{-2} \text{s}^{-1}$. The assimilated ^{14}C was measured as mentioned above. The K_m values of DIC (DIC concentration required for half-maximal photosynthetic rate or half maximal ETR, increased K_m reflects decreased CCM activity) were calculated by fitting the photosynthetic carbon fixation rates and rETR under the PAR level of $400 \mu\text{mol photons m}^{-2} \text{s}^{-1}$ at various DIC concentrations with the Michaelis-Menten formula.

2.5 Measurement of dark respiration

The cells were gently harvested on polycarbonate membrane filters by filtration ($0.22 \mu\text{m}$, Q/YY8-1-88, Xinya), washed

off and then re-suspended in 50 mmol L^{-1} Tris buffered media of pH 8.15 or pH 7.80 (as in the control or acidified cultures) at a final concentration of ca. $2 \times 10^6 \text{ mL}^{-1}$. O_2 consumption was measured with Clark type oxygen electrode (5300A, YSI) at $20 \pm 0.1^\circ\text{C}$, while the reaction vessel (0.8 mL) was completely covered in darkness. No ruptured cells were found in the suspension after filtration.

2.6 Growth rate and chlorophyll-*a* determination

Cell counting was carried out every 24 h with particle count and size analyzer (Z2 Coulter, Beckman) before and after partially renewing the medium. The specific growth rate (μ , d^{-1}) was calculated as: $\mu = (\ln C_1 - \ln C_0) / (t_1 - t_0)$, where C_0 and C_1 represent the cell concentrations at t_0 (initial or just after the dilution) and t_1 (before the dilution), respectively. Chlorophyll-*a* (Chl-*a*) concentration was determined spectrophotometrically as follows:

$$[\text{Chl-}a] = 16.29 \times (A_{665} - A_{750}) - 8.54 \times (A_{652} - A_{750})$$

(Porra, 2002),

where A_{652} , A_{665} and A_{750} represent absorbance of the methanol extracts at 665, 652 and 750 nm, respectively.

2.7 Data analysis

One-way ANOVA and Tukey test were used to establish differences among the treatments ($p = 0.05$). RLC was fitted as $y = x / (ax^2 + bx + c)$ (Eilers and Petters, 1988), where y is the rETR, x is the photon flux density of actinic light ($\mu\text{mol photons m}^{-2} \text{s}^{-1}$), a , b and c are the adjustment parameters. Relative photo-inhibition observed in the RLCs was calculated as $\text{Inh} (\%) = (P_m - P_x) / P_m \times 100\%$, where P_m is the maximal rETR, P_x is the rETR at measuring photon flux density.

3 Results

3.1 Carbonate system

Under the simulated condition for ocean acidification, the carbonate system in the high CO_2 bubbled cultures differed significantly from that of the control (Table 1); DIC, HCO_3^- and CO_2 increased by 8.0%, 11.3%, and 158.5%, while CO_3^{2-} decreased by 50.5%, respectively; the change ($<0.3\%$) of total alkalinity was insignificant. Changes in pH and $p\text{CO}_2$ before and after the partial renewal of the culture medium during the semi-continuous cultures were <0.02 for the former and $<5.8\%$ for the latter.

3.2 Growth, respiration, carbon utilization, and K_m

The cells that had acclimated for 20 generations under the different carbonate systems showed equal content of Chl-*a* (Fig. 1a) of about 0.315 pg per cell, but the specific growth

Table 1. Parameters of the seawater carbonate system under the ambient (39.3 Pa) and enriched (101.3 Pa) CO₂ levels before and after the partial renewal of the medium for the semi-continuous cultures. Dissolved inorganic carbon (DIC), pH, salinity, nutrient concentration, and temperature were used to derive all other parameters using a CO₂ system analyzing software (CO2SYS). Data are the means \pm SD of 9 measurements, the superscripts represent significant difference between ambient and enriched CO₂.

	$p\text{CO}_2$ (Pa)	pH_{NBS}	DIC ($\mu\text{mol kg}^{-1}$)	HCO_3^- ($\mu\text{mol kg}^{-1}$)	CO_3^{2-} ($\mu\text{mol kg}^{-1}$)	CO ₂ ($\mu\text{mol kg}^{-1}$)	Total alkalinity ($\mu\text{mol kg}^{-1}$)
Before	39.3 ± 1.1^a	8.18 ± 0.04^a	1976.2 ± 7.6^a	1768.0 ± 19.8^a	195.7 ± 31.9^a	12.5 ± 1.4^a	2255.9 ± 54.9^a
renewal	101.3 ± 3.0^b	7.82 ± 0.02^b	2137.8 ± 13.2^b	2008.3 ± 12.4^b	97.0 ± 8.2^b	32.4 ± 1.9^b	2251.5 ± 41.5^a
After	39.3 ± 1.1^a	8.16 ± 0.03^a	1998.1 ± 11.5^a	1795.2 ± 4.7^a	189.6 ± 21.8^a	13.3 ± 1.2^a	2273.5 ± 47.7^a
renewal	101.3 ± 3.0^b	7.80 ± 0.02^b	2154.7 ± 15.9^b	2026.9 ± 15.6^b	93.5 ± 8.3^b	34.3 ± 1.9^b	2266.9 ± 44.5^a

Table 2. The rapid light curve fitted parameters (i.e., α , the apparent photochemical efficiency; P_{max} , maximal rETR; I_k , the light saturation point) for low and high CO₂ grown cells, respectively. Derived from Fig. 4, superscripts represent significant difference among treatments.

	α	P_{max}	I_k
L-C	0.293 ± 0.005^a	103.8 ± 1.2^a	353.9 ± 6.9^a
H-C	0.295 ± 0.006^a	103.7 ± 1.4^a	351.5 ± 8.1^a
L-C-H-C	0.288 ± 0.007^a	108.3 ± 1.4^b	376.0 ± 8.0^b
H-C-L-C	0.289 ± 0.008^a	99.9 ± 1.4^c	345.7 ± 8.4^a

rate (μ) was significantly ($p < 0.001$) enhanced by 5.2% under the acidified (high CO₂) condition (Fig. 1b). There was a significant difference in photosynthetic carbon fixation rate between the L-C (low CO₂ grown cells measured in low CO₂) and H-C (high CO₂ grown cells measured in high CO₂), with the latter about 11% higher than the former (Fig. 2a). The photosynthetic carbon fixation rate of L-C-H-C (low CO₂ grown cells measured in high CO₂) was stimulated ($p < 0.00001$) by 17.9% compared to L-C, while that of the H-C-L-C (high CO₂ grown cells measured in low CO₂ at ca. 2.1 mmol L⁻¹ DIC) decreased slightly ($p > 0.05$). Dark respiration of H-C grown cells was 33.7% higher than that of the L-C ($p < 0.02$) (Fig. 2b). The integrated daily carbon fixation during light period and O₂ consumption during dark period were 4.86, 0.86 for L-C and 5.38, 1.15 $\mu\text{mol} (\mu\text{g Chl-}a)^{-1} \text{d}^{-1}$ for H-C (Fig. 2c), leading to higher daily net production (by 5.8%) in the H-C than in the L-C cultures. Under Ci-limited DIC levels ($< 0.5 \text{ mmol L}^{-1}$), the carbon fixation rate and rETR of the H-C grown cells (H-C-L-C) were lower, respectively, by 23% and 10% compared to L-C grown cells (Fig. 3a, b). The K_m (DIC) values, derived either from C-fixation or from rETR P-C curves (Fig. 3c), increased by about 20% for the H-C-L-C cells, reflecting that the photosynthetic Ci affinity was significantly reduced under the low pH and high CO₂ condition.

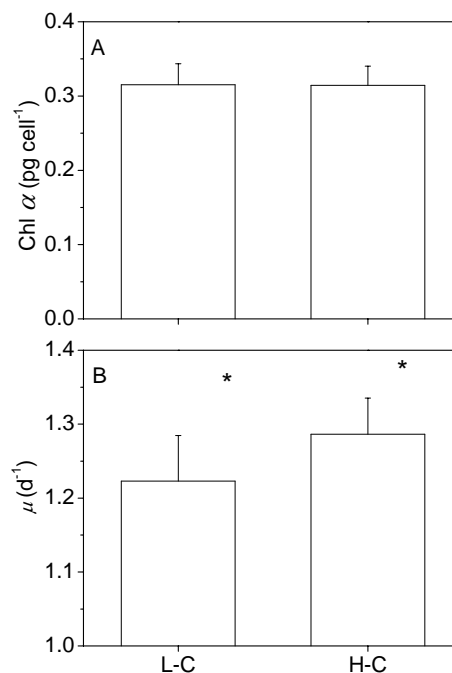


Fig. 1. (A) Cellular chlorophyll-*a* content and (B) specific growth rate (μ), of *P. tricornutum* after 20 generations acclimation to the low (L-C; pH 8.15) and high CO₂ conditions (H-C; pH 7.80). Data are the means \pm SD of 10 and 27 measurements for the Chl-*a* and μ , respectively. An asterisk represents significant difference ($p < 0.001$).

3.3 Photochemical and non-photochemical responses

The light curves measured at pH 8.15 and pH 7.80 (Fig. 4) showed a typical pattern of rETR as a function of PAR. The rETR for L-C-H-C was significantly higher than that for H-C or H-C-L-C under high levels of PAR. The apparent photochemical efficiency (Table 2) was similar for L-C and H-C grown cells, while the maximum rETR was the highest for L-C-H-C, and the lowest for H-C-L-C. Moreover, photo-inhibition was obvious for both the L-C and H-C grown cells

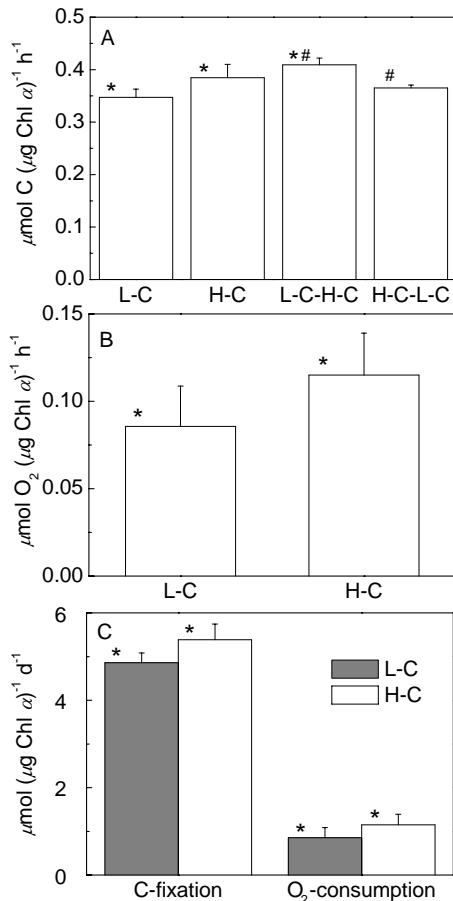


Fig. 2. (A) Photosynthetic carbon fixation, (B) dark respiration, and (C) integrated daily photosynthetic carbon fixation and dark respiration of low (L-C) and high CO₂ grown cells (H-C), low CO₂ grown cells measured in high CO₂ (L-C-H-C) and high CO₂ grown cells measured in low CO₂ (H-C-L-C); vertical bars represent SD, $n = 9-12$ for carbon fixation and 3–5 for oxygen consumption. An asterisk and a number sign “#” represent significant difference among treatments ($p < 0.05$).

(Fig. 4) under high irradiance levels, being the highest in the H-C grown cells, while it was alleviated after transferring into L-C condition.

The yield ratio during the induction curves (Fig. 5a, b) indicates that the CO₂ enrichment stimulated the yield. The H-C grown cells showed higher photochemical activity than L-C by 2.0% and 8.3% under 120 and 840 $\mu\text{mol photons m}^{-2} \text{ s}^{-1}$, respectively, while that of the L-C-H-C was correspondingly higher than H-C-L-C by 5.8% and 12.3%. The non-photochemical quenching (NPQ) increased gradually and reached a constant value in 120 s after turning on the actinic light (Fig. 5c). The H-C grown cells showed lower NPQ, being about 94.3% of that in the L-C grown cells; the NPQ for the H-C-L-C was 82% of the L-C-H-C on average.

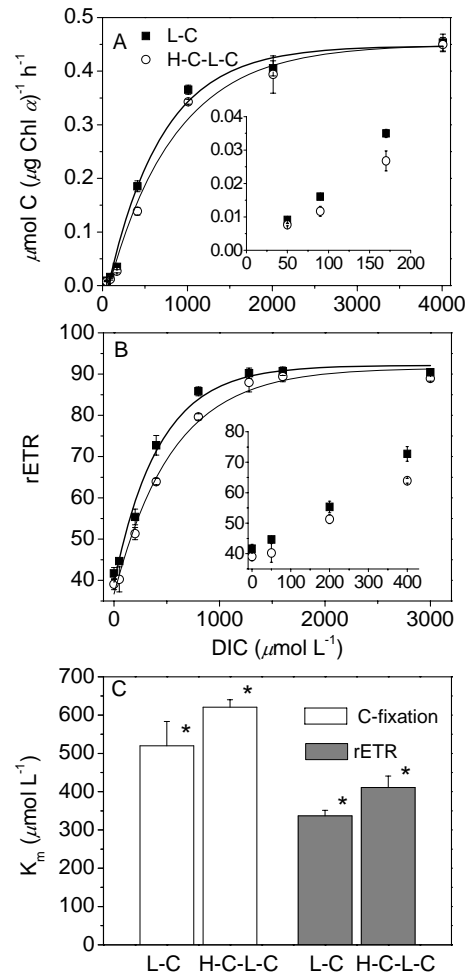


Fig. 3. (A) Photosynthetic carbon fixation rate, (B) rETR under photon flux densities of $400 \mu\text{mol m}^{-2} \text{ s}^{-1}$ as a function of DIC concentration, and (C) the DIC concentrations for the half-maximal photosynthetic rate for cells acclimated and measured under different CO₂ levels (L-C, H-C-L-C as given in legend to Fig. 2). Vertical bars represent SD, $n = 3$.

4 Discussion

It has been a controversial issue whether elevated CO₂ in seawater associated with atmospheric CO₂ rise would significantly promote phytoplankton productivity (see the review by Giordano et al., 2005). Responses of phytoplankton to reduced pH in a high CO₂ ocean are likely to be species-specific, with potential ‘winners’ and ‘losers’ (Hinga, 2002). In the present study, the growth rate of *P. tricornutum* was enhanced by 5.2% under high CO₂ and low pH conditions, the response in photosynthetic carbon fixation was more pronounced (+12%). Since dark respiration was also enhanced, the net daily photosynthetic production was stimulated by 5.8%, which closely agreed with the observed increase in growth. The enhanced respiration, if prevalent in marine organisms in the future high CO₂ and low pH ocean

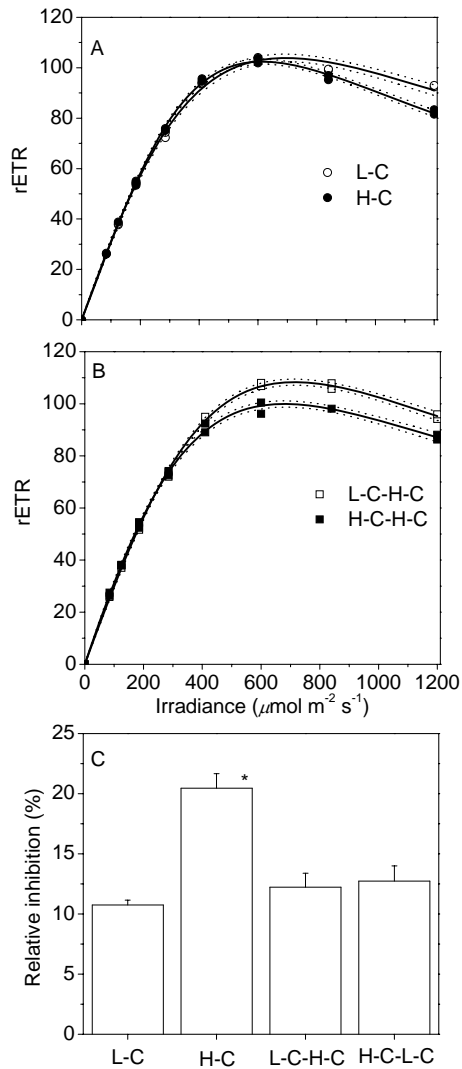


Fig. 4. The rapid light curve of low (L-C) and high CO_2 grown cells (H-C) measured under (A) CO_2 conditions as in their growth medium and (B) measured after transfer to high (L-C-H-C) and low CO_2 levels (H-C-L-C), respectively, and (C) the inhibitions relative to P_m caused by actinic light at $1200 \mu\text{mol m}^{-2} \text{s}^{-1}$. Solid lines represent the best fit of these points, while dotted lines represent 95% confident bands, stars represent significant difference ($p < 0.001$), vertical bars represent SD, $n = 4$.

(Crawley et al., 2010), would couple with seawater warming to consume more gross primary production (del Giorgio and Duarte, 2002). However, increased $p\text{CO}_2$ stimulated carbon fixation by phytoplankton assemblages in a mesocosm study, which led to an increase in the ratio of carbon to nutrient drawdown (Riebesell et al., 2007). The balance of enhanced respiration and excess carbon consumption will determine whether oceanic primary producers will take up less or more CO_2 in the ongoing process of ocean warming and acidification. The enhancement of marine phytoplankton primary productivity associated with atmospheric CO_2 rise was sug-

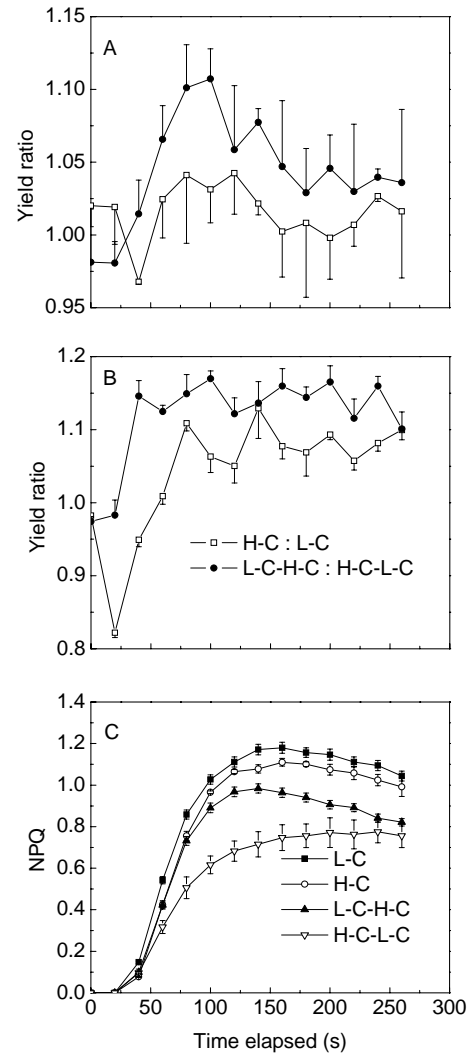


Fig. 5. The effective quantum yield ratios of high (H-C) to low CO_2 grown cells (L-C), that of L-C cells measured in H-C medium (L-C-H-C) to H-C cells measured in L-C medium (H-C-L-C) under (A) 120 and (B) $840 \mu\text{mol m}^{-2} \text{s}^{-1}$, respectively; and (C) non-photochemical quenching (NPQ) under $840 \mu\text{mol m}^{-2} \text{s}^{-1}$ for L-C, H-C, L-C-H-C and H-C-L-C. Vertical bars represent SD, $n = 3$.

gested to be less than 10% (Beardall and Raven, 2004). It has been estimated that marine diatoms fix up to 10 Pg C per year (Granum et al., 2005). If roughly 5% increase in the growth of diatoms were taken into account based on the values obtained in this study, this would allow diatoms to rapidly accumulate more biomass (by about 34% in 6 days) and draw-down available N and other nutrients, leading to a greater biological carbon flux to the deep sea. If other groups of phytoplankton do not show increased growth at elevated CO_2 (unclear for the few that have been studied), diatoms with higher growth rates will outcompete them for nutrients. If the Redfield C:N ratio increase from 6.6 to 7.1 were taken into account as reported in the mesocosm under $2 \times \text{CO}_2$

concentration (Riebesell et al., 2007), provided the nitrogen cell quota remain constant, the diatoms' total carbon fixation would increase even more.

Non-photochemical quenching (NPQ), which consists of three components, qE (energy dependent), qI (photoinhibition dependent), and qT (state transition dependent), is an important mechanism which protects cells from photo-damages and minimizes the production of harmful oxygen radicals (Niyogi et al., 2005). During the transition of dark adapted cells to moderate light conditions, qE is the major component of NPQ induced by thylakoidal acidification (i.e., a high ΔpH) and functions in thermal dissipation of excessive light energy for PSII, thus reducing electron pressure in the electron transport chain (Niyogi et al., 2005). In the present study, simulated ocean acidification enhanced photo-inhibition of ETR, but led to down-regulation of the CCM and reduction of NPQ. Since the adenosine triphosphate (ATP) generation by trans-membrane H^+ -ATPase will reduce the thylakoidal acidification, the enhanced carboxylation due to the enrichment of CO_2 would have consumed more ATP, drained H^+ out of the lumen and then decreased NPQ (Kanazawa and Kramer, 2002). Lower NPQ might also be attributed to the down-regulation of CCM which functions to concentrate intracellular CO_2 and subsequently acidify the thylakoid lumen (Raven, 1997). However, operation of the CCM can play a role in draining the electrons and lead to reduced photoinhibition (Qiu and Liu, 2004). The down-regulated CCM of *P. tricornutum* grown at high CO_2 could be associated with weakened cyclic electron transport (Moroney and Somanchi, 1999) that can also lead to higher photo-inhibition (Takahashi et al., 2009). Overall, the decreased NPQ represents a net result of the lowered qE over the enhanced qI under the acidified and CO_2 -enriched condition.

While the ongoing ocean acidification has been shown to adversely affect calcifying marine organisms (Riebesell et al., 2000; Gao and Zheng, 2010) though stimulated productivity was observed (Iglesias-Rodriguez et al., 2008), it can also be a potential stress on non-calcifying organisms. When the L-C-grown cells were transferred to H-C and had grown for 20 generations, the photo-inhibition of ETR increased. However, when these H-C grown cells were transferred back to the L-C medium, their photo-inhibition of ETR decreased immediately (Fig. 4) and relaxation of NPQ was observed (Fig. 5). Such changes might be due to an immediate enhancement of cyclic electron transport due to activation of CCM associated with the removal of pH stress and reduction in CO_2 availability. Nevertheless, the apparent photochemical efficiency was equivalent between the two kinds of cells (Table 2), reflecting comparable energetic cost for the light-limited photosynthesis. However, it is hard to conclude that the energetic cost of carbon concentration in *Phaeodactylum tricornutum* is small. The cells grown under elevated CO_2 in the low-pH culture can save some energy due to down-regulation of CCM, but at the same time, they need addi-

tional energy to cope with external pH decrease. When the actinic light intensity was elevated, the more efficiently operated CCM in the low- CO_2 grown cells consumed more energy, while the high- CO_2 grown cells with down regulated CCM saved energy that causes photoinhibition to increase (Fig. 4). Meanwhile, the enhanced dark respiration under lowered pH could reflect higher energy demand due to either increased biosynthesis in response to enhanced carbon fixation or higher energy requirement to counteract the external pH reduction (Geider and Osborne, 1989). Since transferring the L-C grown cells into the H-C medium did not immediately induce higher photo-inhibition, the physiological response to the pH change can hardly be instant but inducible during acclimation.

While cells exposed to moderate light intensities (PAR $\sim 120 \mu\text{mol photons m}^{-2} \text{s}^{-1}$) appeared to benefit from elevated CO_2 availability when grown under high CO_2 and low pH conditions, leading to increased photosynthetic carbon fixation and enhanced growth rate in *P. tricornutum*, cells exposed to excessive light levels appeared to suffer more damage to PSII in the high compared to the L-C grown cells. Hence, ocean acidification is likely to have different impacts on cells suspended in the immediate surface layer compared to those in deeper layers of the water column, and may lead to less photosynthetic production in the upper layer of euphotic zone. Since phytoplankton cells are also susceptible to solar UV radiation in their natural environment (Gao et al., 2007), their physiology may be synergistically affected by UV and ocean acidification (Sobrinho et al., 2008). While UV-A was also found to enhance photosynthetic carbon fixation (Gao et al., 2007) of phytoplankton assemblages and growth of a cyanobacterium (Wu et al., 2005), the change of water column primary productivity is uncertain due to the scarce knowledge on the combined effects of acidification and solar radiation in the euphotic zone.

Based on the results from the present study, the ongoing ocean acidification may cause diatoms to increase growth, down-regulate their CCM, and experience enhanced photo-inhibition and dark respiration. The balance between these positive and negative effects on diatom productivity will be a key factor in determining the net effect of rising atmospheric CO_2 on ocean primary production. Down-regulation of CCMs and consequently related changes in photochemical processes in diatoms can be expected to occur with the continuing ocean acidification. In view of the diversified phytoplankton species and their physiology, the apparent species-specific response of phytoplankton to changes in seawater carbonate system associated with ocean acidification might lead to alteration of present competitions among phytoplankton species (Falkowski and Oliver, 2007) and even to differential evolution of phytoplankton taxa (Collins and Bell, 2004).

Acknowledgements. This study was funded by National Basic Research Program of China (2009CB421207 to KG) and National Natural Science Foundation of China (40930846 and 40876058 to KG). Ulf Riebesell was supported by the visiting professor program (111) from the ministry of Education.

Edited by: J. Middelburg

References

- Badger, M. R., Andrews, T. J., Whitney, S. M., Ludwig, M., Yel-lowlees, D. C., Leggat, W., and Price, G. D.: The diversity and coevolution of Rubisco, plastids, pyrenoids, and chloroplast-based CO₂-concentrating mechanisms in algae, *Can. J. Botany*, 76, 1052–1071, 1998.
- Barry, J. P., Tyrrell, T., Hansson, L., and Gattuso, J.-P.: Atmospheric CO₂ targets for ocean acidification perturbation experiments, in: Guide to best practices in ocean acidification research and data reporting, edited by: Riebesell, U., Fabry, V. J., Hansson, L., and Gattuso, J.-P., Publications Office of the European Union, Luxembourg, 2010.
- Beardall, J. and Raven, J. A.: The potential effects of global climate change on microalgal photosynthesis, growth and ecology, *Phycologia*, 43, 26–40, 2004.
- Burkhardt, S., Amoroso, G., Riebesell, U., and Sultermeyer, D.: CO₂ and HCO₃⁻ uptake in marine diatoms acclimated to different CO₂ concentrations, *Limnol. Oceanogr.*, 46, 1378–1391, 2001.
- Burkhardt, S., Zondervan, I., and Riebesell, U.: Effect of CO₂ concentration on C: N: P ratio in marine phytoplankton: A species comparison, *Limnol. Oceanogr.*, 44, 683–690, 1999.
- Caldeira, K. and Wickett, M. E.: Anthropogenic carbon and ocean pH, *Nature*, 425, p. 365, 2003.
- Collins, S. and Bell, G.: Phenotypic consequences of 1000 generations of selection at elevated CO₂ in a green alga, *Nature*, 431, 566–569, 2004.
- Conley, D. J., Kilham, S. S., and Theriot, E.: Differences in silica content between marine and freshwater diatoms, *Limnol. Oceanogr.*, 34, 205–213, 1989.
- Crawley, A., Kline, D. I., Dunn, S., Anthony, K., and Dove, S.: The effect of ocean acidification on symbiont photorespiration and productivity in *Acropora formosa*, *Glob. Change Biol.*, 16, 851–863, 2010.
- del Giorgio, P. A. and Duarte, C. M.: Respiration in the open ocean, *Nature*, 420, 379–384, 2002.
- Dickson, A. G.: Standard potential of the reaction: AgCl(s) + 1/2 H₂(g) = Ag(s) + HCl(aq), and the standard acidity constant of the ion HSO₄⁻ in synthetic seawater from 273.15 to 318.15 K, *J. Chem. Thermodyn.*, 22, 113–127, 1990.
- Doney, S. C., Fabry, V. J., Feely, R. A., and Kleypas, J. A.: Ocean Acidification: the other CO₂ problem, *Annu. Rev. Mar. Sci.*, 1, 169–192, 2009.
- Eilers, P. H. C. and Petters, J. C. H.: A model for the relationship between light intensity and the rate of photosynthesis in phytoplankton, *Ecol. Model.*, 42, 199–215, 1988.
- Falkowski, P. G. and Oliver, M. J.: Mix and match: how climate selects phytoplankton, *Nat. Rev. Microbiol.*, 5, 813–819, 2007.
- Gao, K., Aruga, Y., Asada, K., Ishihara, T., Akano, T., and Kiyohara, M.: Calcification in the articulated coralline alga *Corallina pilulifera*, with special reference to the effect of elevated CO₂ concentration, *Mar. Biol.*, 117, 129–132, 1993.
- Gao, K., Wu, Y., Li, G., Wu, H., Villafañe, V. E., and Helbling, E. W.: Solar UV-radiation drives CO₂-fixation in marine phytoplankton: a double-edged sword., *Plant Physiol.*, 144, 54–59, 2007.
- Gao, K. and Zheng, Y.: Combined effects of ocean acidification and solar UV radiation on photosynthesis, growth, pigmentation and calcification of the coralline alga *Corallina sessilis* (Rhodophyta), *Glob. Change Biol.*, 16, 2388–2398, doi:10.1111/j.1365-2486.2009.02113.x, 2010.
- Geider, R. J. and Osborne, B. A.: Respiration and microalgal growth: a review of the quantitative relationship between dark respiration and growth, *New Phytol.*, 112, 327–341, 1989.
- Giordano, M., Beardall, J., and Raven, J. A.: CO₂ concentrating mechanisms in algae: mechanisms, environmental modulation, and evolution, *Annu. Rev. Plant Biol.*, 56, 99–131, 2005.
- Granum, E., Raven, J. A., and Leegood, R. C.: How do marine diatoms fix 10 billion tonnes of inorganic carbon per year?, *Can. J. Bot.*, 83, 898–908, 2005.
- Hein, M. and Sand-Jensen, K.: CO₂ increases oceanic primary production, *Nature*, 388, 526–527, 1997.
- Hester, K. C., Peltzer, E. T., Kirkwood, W. J., and Brewer, P. G.: Unanticipated consequences of ocean acidification: a noisier ocean at lower pH, *Geophys. Res. Lett.*, 35, L19601, doi:10.1029/2008GL034913, 2008.
- Hinga, K. R.: Effects of pH on coastal marine phytoplankton, *Mar. Ecol.-Prog. Ser.*, 238, 281–300, 2002.
- Hoegh-Guldberg, O., Mumby, P. J., Hooten, A. J., Steneck, R. S., Greenfield, P., Gomez, E., Harvell, C. D., Sale, P. F., Edwards, A. J., Caldeira, K., Knowlton, N., Eakin, C. M., Iglesias-Prieto, R., Muthiga, N., Bradbury, R. H., Dubi, A., and Hatziolos, M. E.: Coral reefs under rapid climate change and ocean acidification, *Science*, 318, 1737–1742, 2007.
- Iglesias-Rodriguez, M. D., Halloran, P. R., Rickaby, R. E. M., Hall, I. R., Colmenero-Hidalgo, E., Gittins, J. R., Green, D. R. H., Tyrrell, T., Gibbs, S. J., von Dassow, P., Rehm, E., Armbrust, E. V., and Boessenkool, K. P.: Phytoplankton calcification in a high-CO₂ world, *Science*, 320, 336–340, 2008.
- Kanazawa, A. and Kramer, D. M.: In vivo modulation of nonphotochemical exciton quenching (NPQ) by regulation of the chloroplast ATP synthase, *P. Natl. Acad. Sci. USA*, 99, 12789–12794, 2002.
- Lewis, E. and Wallace, D. W. R.: Program Developed for CO₂ System Calculations, ORNL/CDIAC-105, Carbon Dioxide Information Analysis Center, Oak Ridge National Laboratory, US Department of Energy, 1998.
- Morel, F. M. M., Rueter, J. G., Anderson, D. M., and Guillard, R. R. L.: Aquil: a chemically defined phytoplankton culture medium for trace metal studies, *J. Phycol.*, 15, 135–141, 1979.
- Moroney, J. V. and Somanchi, A.: How do algae concentrate CO₂ to increase the efficiency of photosynthetic carbon fixation?, *Plant Physiol.*, 119, 9–16, doi:10.1104/pp.119.1.9, 1999.
- Niyogi, K. K., Li, X. P., Rosenberg, V., and Jung, H. S.: Is PsbS the site of non-photochemical quenching in photosynthesis?, *J. Exp. Bot.*, 56, 375–382, 2005.
- Orr, J. C., Fabry, V. J., Aumont, O., Bopp, L., Doney, S. C., Feely, R. A., Gnanadesikan, A., Gruber, N., Ishida, A., Joos, F., Key, R. M., Lindsay, K., Maier-Reimer, E., Matear, R., Monfray, P.,

- Mouchet, A., Najjar, R. G., Plattner, G. K., Rodgers, K. B., Sabine, C. L., Sarmiento, J. L., Schlitzer, R., Slater, R. D., Totterdell, I. J., Weirig, M. F., Yamanaka, Y., and Yool, A.: Anthropogenic ocean acidification over the twenty-first century and its impact on calcifying organisms, *Nature*, 437, 681–686, 2005.
- Porra, R. J.: The chequered history of the development and use of simultaneous equations for the accurate determination of chlorophylls a and b, *Photosynth. Res.*, 73, 149–156, 2002.
- Qiu, B. S. and Liu, J. Y.: Utilization of inorganic carbon in the edible cyanobacterium Ge-Xian-Mi (*Nostoc*) and its role in alleviating photo-inhibition, *Plant Cell Environ.*, 27, 1447–1458, 2004.
- Raven, J. A.: CO₂-concentrating mechanisms: a direct role for thylakoid lumen acidification?, *Plant Cell Environ.*, 20, 147–154, 1997.
- Riebesell, U., Wolf-Gladrow, D. A., and Smetacek, V. S.: Carbon dioxide limitation of marine phytoplankton growth rates, *Nature*, 361, 249–251, 1993.
- Riebesell, U., Zondervan, I., Rost, B., Tortell, P. D., Zeebe, R. E., and Morel, F. M. M.: Reduced calcification of marine plankton in response to increased atmospheric CO₂, *Nature*, 407, 364–367, 2000.
- Riebesell, U., Schulz, K. G., Bellerby, R. G. J., Botros, M., Fritsche, P., Meyerhofer, M., Neill, C., Nondal, G., Oschlies, A., Wohlers, J., and Zollner, E.: Enhanced biological carbon consumption in a high CO₂ ocean, *Nature*, 450, 545–549, 2007.
- Rost, B., Riebesell, U., Burkhardt, S., and Sultemeyer, D.: Carbon acquisition of bloom-forming marine phytoplankton, *Limnol. Oceanogr.*, 48, 55–67, 2003.
- Roy, R. N., Roy, L. N., Vogel, K. M., Porter-Moore, C., Pearson, T., Good, C. E., Millero, F. J., and Campbell, D. M.: The dissociation constants of carbonic acid in seawater at salinities 5 to 45 and temperature 0 to 45 °C, *Mar. Chem.*, 44, 249–267, 1993.
- Sabine, C. L., Feely, R. A., Gruber, N., Key, R. M., Lee, K., Bullister, J. L., Wanninkhof, R., Wong, C. S., Wallace, D. W., Tilbrook, B., Millero, F. J., Peng, T. H., Kozyr, A., Ono, T., and Rios, A. F.: The oceanic sink for anthropogenic CO₂, *Science*, 305, 367–371, 2004.
- Sobrinho, C., Ward, M. L., and Neale, P. J.: Acclimation to elevated carbon dioxide and ultraviolet radiation in the diatom *Thalassiosira pseudonana*: Effects on growth, photosynthesis, and spectral sensitivity of photoinhibition, *Limnol. Oceanogr.*, 53, 494–505, 2008.
- Takahashi, S., Milward, S. E., Fan, D.-Y., Chow, W. S., and Badger, M. R.: How does cyclic electron flow alleviate photoinhibition in *Arabidopsis*?, *Plant Physiol.*, 149, 1560–1567, doi:10.1104/pp.108.134122, 2009.
- Wu, H., Gao, K., Ma, Z., and Watanabe, T.: Effects of solar ultraviolet radiation on biomass production and pigment contents of *Spirulina platensis* in commercial operations under sunny and cloudy weather conditions, *Fisheries Sci.*, 71, 454–456, 2005.
- Xiang, Y. B., Zhang, J., and Weeks, D. P.: The Cia5 gene controls formation of the carbon concentrating mechanism in *Chlamydomonas reinhardtii*, *P. Natl. Acad. Sci. USA*, 98, 5341–5346, 2001.